

PAPER

Localizing and inducing primary nucleation

Zoubida Hammadi,^a Romain Grossier,^a Shuheng Zhang,^a Aziza Ikni,^b Nadine Candoni,^a Roger Morin^a and Stéphane Veessler^{*a}

Received 22nd December 2014, Accepted 27th January 2015

DOI: 10.1039/c4fd00274a

Do the differing properties of materials influence their nucleation mechanisms? We present different experimental approaches to study and control nucleation, and shed light on some of the factors affecting the nucleation process.

Introduction

With the control of material properties being directly related to their methods of production, understanding the mechanisms governing these methods is vital. With crystallized materials, such as minerals, pharmaceuticals, proteins, biominerals and nanomaterials, the most important properties of crystal morphology, habit, size distribution and phases are controlled by the nucleation step. Nucleation was clearly defined by D. Kashchiev as “the process of random generation of those nanoscopically small formations of the new phase that have the ability for irreversible overgrowth to macroscopic sizes”.¹ The size of the critical cluster and the nucleation rate are determined by the classical nucleation theory (CNT) derived from the Gibbs treatment of droplet nucleation.² Interestingly, this simple model fits experimental results very well but is many orders of magnitude out in predicting nucleation frequencies, as shown with protein crystallization.³ It is noteworthy that even experimental data on the same system, in the same conditions, can have discrepancies of more than 10 orders of magnitude,^{3–7} as illustrated in Fig. 1.

Moreover, in several studies on protein crystallization using solution scattering techniques, ultracentrifugation–sedimentation and dialysis kinetics, data were interpreted as indicating the formation of prenucleation aggregates, clusters or oligomeric species, ranging between monomer and crystal.^{8–19} However, other authors^{20–26} did not observe such aggregates and offered the following explanation: “the failure to account for direct and indirect protein interactions in the solutions results in unrealistic aggregation scenarios”.²³ Note that the stable entity in solution is not necessarily a monomer; it can be an oligomer, for

^aCINaM-CNRS, Aix-Marseille Université, Campus de Luminy, F-13288 Marseille, France. E-mail: veessler@cinam.univ-mrs.fr

^bSPMS-CNRS, UMR 8580, Grande Voie des Vignes, F-92295 Châtenay-Malabry, France

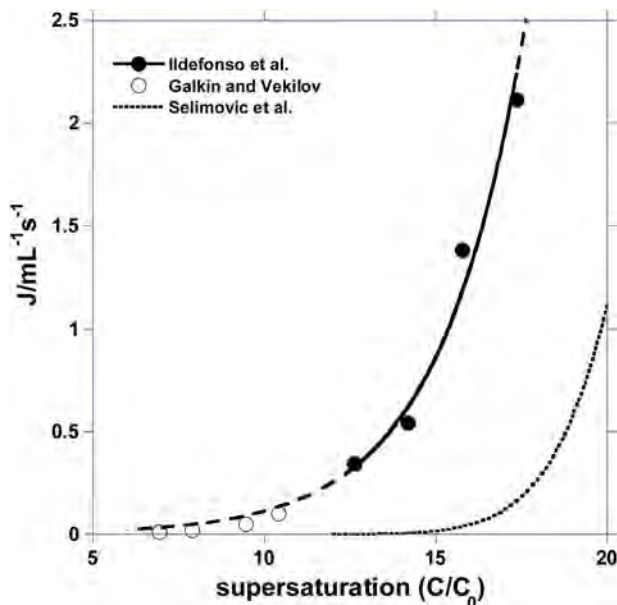


Fig. 1 Primary nucleation rate of lysozyme vs. supersaturation: (●) data at $20\text{ }^\circ\text{C}$ - $C_0 = 3.2\text{ mg mL}^{-1}$ ($\text{NaCl} = 0.7\text{ M}$ and $\text{pH} = 4.5$) from Ildefonso *et al.* in microfluidics,⁴⁴ (○) data, at $12.6\text{ }^\circ\text{C}$ - $C_0 = 1.6\text{ mg mL}^{-1}$ ($\text{NaCl} = 0.7\text{ M}$ and $\text{pH} = 4.5$), from Galkin and Vekilov in microbatches in oil⁷ and (...) data at $12\text{ }^\circ\text{C}$ - $C_0 = 5\text{ mg mL}^{-1}$ ($\text{NaCl} = 0.6\text{ M}$ and $\text{pH} = 4.5$) from Selimovic *et al.* in microfluidics.⁴

biological or physicochemical reasons.²⁷ Finally, simulation papers published in the same period proposed a 2-step process for protein crystal nucleation^{28–30} using the presence of a metastable LLPS (liquid–liquid phase separation) to reduce the nucleation free-energy barrier. The first step could be a local densification (liquid-like dense phase) and the second step could be the nucleation of the solid inside this dense phase. There has even been a third nucleation pathway proposed, linked to biomineralization, consisting of nucleation *via* stable prenucleation clusters.³¹

To summarize, in the CNT only one order parameter, density, describes the transition between the two phases, whereas in the 2-step theory two order parameters, density and structure, are used. For reviews see ref. 32 and 33. This appears to us as an attempt to find a universally applicable explanation for experimental discrepancies. Firstly, the limiting step, densification or structuration, will depend on the solute, as suggested by Knezic *et al.*³⁴ For example, macromolecules take longer to rearrange themselves into crystalline nuclei than smaller molecules. Secondly, the fact that the location, nature and lifetime of the dense phase and/or the critical nucleus are unknown (at the moment) explains difficulties encountered in experimental observations and interpretations. In this paper, however, we explore nucleation from a purely practical point of view, without any *a priori* assumption on the nucleation mechanism. We describe the two experimental approaches taken here: indirect experiments, measuring nucleation frequency by counting crystals or by measuring induction time, and direct experiments, observing the critical nucleus. Kinetic measurements will

provide us with data to be tested by classical and 2-step nucleation models.³⁵ Meanwhile, direct observation will yield information on the size and structure of the critical nucleus. The objective is to shed light on nucleation mechanisms in solution.

Experimental

I. Microfluidic set-up (~nL)

Experiments were performed in PDMS (poly(dimethylsiloxane)) and PEEK (polyether ether ketone) and Teflon devices based on HPLC techniques; T-shaped junctions as described previously^{36,37} or cross-shaped (Zhang *et al.* submitted) (“plug-factory”) were used to form the droplets with volumes in the nanoliter range, without the addition of surfactants. We used FMS oil (Hampton Research) for aqueous solvents. This oil shows no or very low miscibility with water and good wettability with PDMS and Teflon. The droplet concentration and composition were varied using a programmable multi-channel syringe pump (neMESYS) and by controlling the relative and absolute flow rates of the different solutions. (Zhang *et al.* submitted) The tubing containing the droplets was placed in a thermostatted tubing-holder and incubated to obtain crystallization. Droplets were observed using an XYZ-motorized camera.

II. Production of microdroplets with microinjectors (~pL to fL)

We used a simply-constructed and easy-to-use fluidic device that generates arrayed aqueous phase microdroplets in oil, with volumes ranging from nanoliter to femtoliter, without the addition of surfactant.³⁸ The device enables the entire volume range to be attained in the course of one experiment. All experiments were performed on a hydrophobic coverslip, at 20 °C in a thermostatted room. The coverslip was covered with approximately 100 μ L of inert DMS oil (Hampton Research HR3-419, refractive index = 1.390). The micrometer-sized droplets of water solution were generated on the coverslip by a microinjector (Femtojet Eppendorf) with a micropipette of 0.5 μ m internal diameter (Femtotip Eppendorf). Two home-made micromanipulators (MS30 Mechanics) consisting of 3 miniature translation stages allowed displacement of the injector (capillary holder) and the tip in X, Y and Z, with a displacement of 18 mm in the 3 directions by steps of 16 nm. Here, we made the sharp tips from tungsten (W) wires (125 μ m diameter); for a detailed description see ref. 39–41.

III. Localized DC electric field

The experimental set-up was composed of a crystallization cell with two electrodes, at least one of which had a sharp W-tip, as previously described.⁴¹ Two home-made micromanipulators allowing displacement of the electrodes in X, Y and Z were added.

IV. Protein solutions

Hen-egg white lysozyme (14 600 Da, pI = 11.2) was purchased from Sigma (batch 057K7013 L 2879) and used without further purification. The purity of lysozyme was checked by molecular sieving. Proper amounts of lysozyme and NaCl were dissolved in pure water (ELGA UHQ reverse osmosis system) to obtain the

necessary stock solutions. The different solutions were buffered with 80 mM acetic acid, adjusted to pH = 4.5 with NaOH (1 M) and filtered through 0.22 μm Millipore filters. The pH was checked with a pH meter (Schott Instrument, Prolab 1000) equipped with a pH microelectrode. Lysozyme concentrations were checked by optical density measurements (Shumadzu, UV-1800) using an extinction coefficient of $2.64 \text{ mL cm}^{-1} \text{ mg}^{-1}$ at 280 nm for lysozyme.

V. Gel solutions

A stock solution of 1% agarose type V from Sigma (gel point $42 \text{ }^\circ\text{C}$) was prepared using the method developed by Robert and Lefaucheu. ⁴² Gel lysozyme solutions were prepared by mixing at $42 \text{ }^\circ\text{C}$ the solutions of agarose gel, sodium chloride and protein, yielding a final agarose concentration of 1% w/v. The mixture gelled in a few minutes once the temperature was decreased.

VI. Mineral solutions

NaCl (R.P. Normapur, analytical reagent) solutions were prepared by dissolution of the proper amount of powder in pure water.

VII. Oils

Dodecanemethylpentasiloxane (DMS) oil (Hampton Research HR2-593, refractive index = 1.390 at $20 \text{ }^\circ\text{C}$) and paraffin oil (Hampton Research HR3-421, refractive index = 1.467) were used as continuous phases.

Results and discussions

I. Indirect experiments

The indirect measurement of nucleation is obtained through nucleation frequencies or induction times. Because nucleation has a stochastic nature, it is important to perform a large number of experiments, in order to obtain reliable data. Here nucleation was performed in small volumes, in order to reduce the number of crystals and to render their observation easier. Moreover, this has the advantage of decreasing the quantity of molecules while speeding up heat and mass transfer. ⁴³ In addition, the supersaturation range experimentally accessible is increased for kinetic ⁴⁴ and thermodynamic ⁴⁵ reasons. One kinetic limitation in small volumes arises from the nucleation frequency (J /number of nucleus by unit time and volume): the smaller the volume, the longer the induction time and the wider the metastable zone, thus requiring greater supersaturation for nucleation. ^{46,47}

I.1. Small volumes of μL to nL range, the kinetic effect. Our experiments used microfluidics technologies. Microfluidics has proved an efficient way of measuring nucleation frequency, by measuring the probability of crystal presence in the droplets as a function of time ⁴⁸⁻⁵⁰ and by counting the number of crystal nuclei per droplet. ⁴⁴ Fig. 1 summarizes data from different studies obtained using the double pulse technique. ^{6,51,52} This technique allows direct determination of the steady-state rate of primary nucleation, separating crystal nucleation from the growth process, by counting nucleated crystals instead of estimating the induction times. The discrepancies between the data presented in Fig. 1 chiefly stem from the experimental method applied, where the supersaturation during

the quench is not constant, according to the authors.⁴ Note the agreement between data obtained in microbatches⁷ ($\sim 1 \mu\text{L}$) and microfluidics⁴⁴ ($\sim 100 \text{ nL}$). When the volume is diminished, the range of experimentally measurable J is increased. One of the limitations usually involved in measuring J is the supersaturation range over which the experiment can be performed. When β is too low, nucleation frequency is low and nucleation is sensitive to local heterogeneity. When β is too high, J is difficult to measure because it is too rapid. This is why in practice, we are only able to measure the nucleation frequency in the vicinity of the metastable zone limit.

I.2. Small volumes of pL range, the thermodynamic effect. Emulsion-based methods such as microfluidics have advantages; they permit the production, storage and observation of a large number of microdroplets of controlled chemical composition, for instance. But microfluidics has also drawbacks: microdroplet size is controlled by channel size and the microdroplets are not accessible (hardware limitation). Microdroplet generation with micropipettes or microinjectors render microdroplets accessible and makes the size range easy to control. However, its drawback is that a single microdroplet is produced.^{43,53,54} Consequently, we recently presented a fluidic device³⁸ that generates arrayed aqueous phase microdroplets under oil (sessile geometry). This set-up combines the advantage of channelled microfluidic techniques, generating thousands of droplets (Fig. 2), with the advantage of micropipette techniques, giving control over size and microdroplet accessibility.

As pointed out by Bempah and Hileman,⁵⁵ “One major problem associated with the use of the droplet technique in nucleation studies is the creation of sufficient supersaturation within each droplet to ensure crystallization”. In other words, the smaller the volume, the longer the induction time and the wider the metastable zone. Hence a thermodynamic limitation appears because, contrary to CNT which supposes an infinite reservoir of molecules, supersaturation is no longer constant during the nucleation process (aggregation of molecules) but is decreasing.⁴⁵ In these small-volume systems, unexpected high-supersaturated metastable solutions are observed. In practice, there is an influence of the volume on nucleation from a picoliter range down.⁴⁵ This is in agreement with experimental results showing effects under nanoscopic confinement.^{56–60}

We therefore used the droplet contraction method to generate sufficient supersaturation, *i.e.* diffusion of water from the microdroplet into the oil. The experiment presented in Fig. 3 and 4 is isothermal ($20 \text{ }^\circ\text{C}$) and the volume is decreasing linearly⁶¹ with time and can be monitored throughout the experiment.



Fig. 2 Array of droplets (~ 720) of NaCl solutions generated through the layer of inert DMS oil.

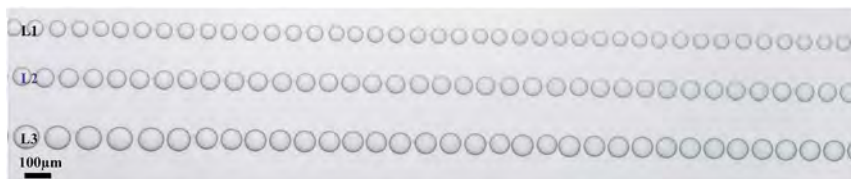


Fig. 3 Array of droplets of NaCl solutions at $\beta = 0.1$ generated through the layer of inert DMS oil. Microdroplet volumes are 104, 172 and 284 pL for rows L1, L2 and L3 respectively, 104 pL assuming a spherical shape for the droplet with a contact angle of 130° as measured previously.⁶¹

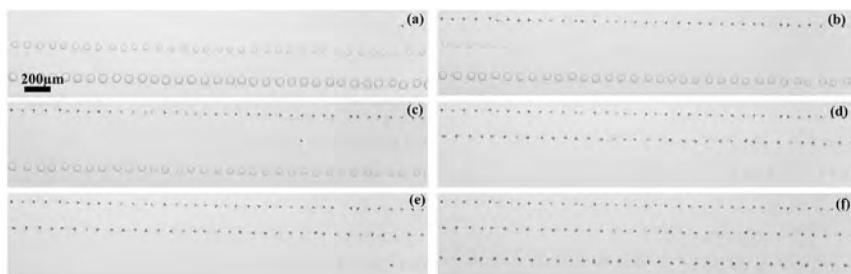


Fig. 4 Time sequence showing nucleation of NaCl crystals (a) at $t = 1106$ s, (b) $t = 1305$ s and (c) $t = 1390$ s, (d) at $t = 1563$ s, (e) $t = 1680$ s and (f) $t = 1995$ s. In (a), (c) and (e) the first microdroplet in L1, L2 and L3 has crystallized and in (b), (d) and (f) all microdroplets in L1, L2 and L3 have crystallized. All micrographs are at the same magnification. Rows L1, L2 and L3 are from Fig. 3.

In the first stage (Fig. 3), 3 microdroplet rows containing NaCl solution at $\beta = 0.1$ are generated, and supersaturation β is defined as the ratio of the NaCl concentration in solution *versus* the solubility of NaCl, 6.15 M at 20°C in water.⁶² Droplets slowly evaporate until critical supersaturation is reached. The critical supersaturation for nucleation is the maximum supersaturation that a solution can withstand without nucleating a new phase.⁴⁷ The nucleation times of the microdroplets from the experiment (Fig. 3 and 4) are plotted in Fig. 5, where $P(t)$ represents the normalized fraction of nucleated microdroplets. Due to the fast growth rate, the time required for the newly-formed nuclei to grow to a detectable size is negligible with regards to the induction time (see Fig. 6). Thus, the time when a detectable crystal is observed can be considered the induction time. In the experiment shown in Fig. 3 and 4, we observe that the smaller the volume, the faster the evaporation rate and the faster the nucleation (Fig. 5).

II. Direct experiments

According to Davey *et al.*,⁶³ “The biggest challenge is to identify the structure of low-concentration, nanosized dynamic clusters of molecules”. Thus, with the development of new experimental tools such as *in situ* electron microscopy,⁶⁴ cryogenic transmission electron microscopy,^{65,66} fluctuation transmission electron microscopy,⁶⁷ AFM,⁶⁸ laser scanning confocal microscopy,⁶⁹ laser confocal

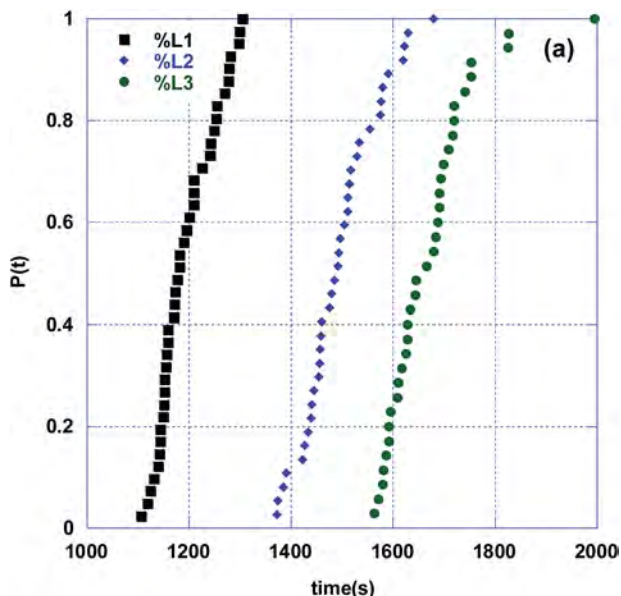


Fig. 5 Nucleation probability $P(t)$ vs. time. $P(t)$ represent the normalized fraction of nucleated microdroplets. Rows L1, L2 and L3 are from Fig. 3.

differential interference contrast microscopy⁷⁰ or even classical microscopy for colloidal nucleation,⁷¹ an increasing focus is placed on how to catch the critical cluster. The challenge is that nucleation is stochastic: during an experiment, we do not know where and when nucleation will occur. All we can do in our different laboratories, for the moment, is to perform many experiments and hope that the law of large numbers will allow us to observe critical clusters. Whether or not this experimental observation is representative of nucleation is still an open question (see the controversy over the existence of prenucleation aggregates).

II.1. Confinement by volume and external field. Here, we address the unpredictability of the spatial and temporal location of the critical nucleus. In the experiment presented in Fig. 3 and 4, confinement by volume allows us to have spatial control at the picoliter scale. With this set-up, a resolution better than 1 μm would be difficult to obtain, which is still far from the expected size of a critical cluster.

Thus, we propose confinement coupled to an external field, in order to control the location of the nucleation event. The implications of an external field for crystal growth in solution were highlighted by Voss,⁷² Oxtoby⁷³ and Revalor.⁵² Two effects on the supersaturated solutions are expected: molecular orientation and density fluctuation. The principle of the experiment is that first solute microdroplets are generated in oil with the microinjector, and the microdroplets then concentrate contraction to generate supersaturation. Secondly, when the microdroplets completely disappear a sharp tip is used to induce a nucleation event, by touching the supersaturated metastable microdroplet.

It was previously shown that any disturbance, for instance a crystal touching dense droplets⁷⁴ or mechanical contact with a nanotip,⁷⁵ triggers nucleation. In

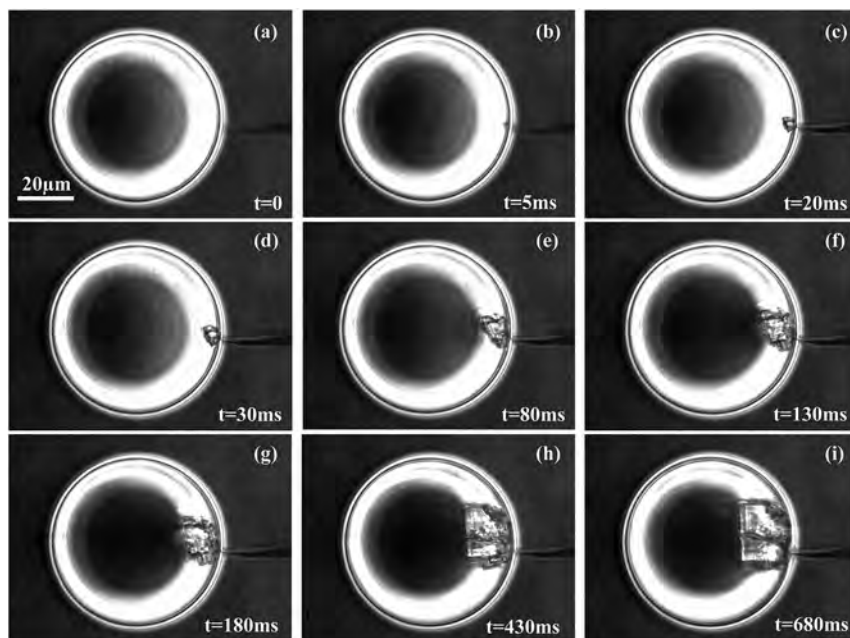


Fig. 6 Panels representing a time sequence showing nucleation induced by a sharp tip and growth of NaCl in paraffin oil. (a) Initial condition: $\beta > 1.24$, (a) droplet size $60 \mu\text{m}$ (95 pL assuming a spherical shape for the droplet with a contact angle of 120° at the time of nucleation as measured previously⁶¹). All micrographs (phase contrast mode) are at the same magnification.

the experiment presented in Fig. 6, we induced a structural transformation *via* mechanical contact at precisely determined points (at 16 nm accuracy) and times, using an sCMOS camera at 200 frames per s (Andeor Neo). The time between tip contact and observation of nucleation was shorter than 5 ms (Fig. 6a and b) and the mean crystal growth rate was greater than $200 \mu\text{m s}^{-1}$ during the first 20 ms (Fig. 6a–c). The nucleated crystal was rough, and transition to a faceted crystal was observed in less than 1 s, *i.e.* the transition between the nucleation form and the equilibrium form. In practice, because the tip position is controlled with micro-manipulators, the position of the critical nucleus can be determined with an accuracy of 16 nm.

This method has some drawbacks, however. First, it is a trial and error method: the droplet is repeatedly tapped with the tip during the generation of supersaturation by water diffusion in order to launch nucleation. Second, it is less successful with protein, probably because the crystallization medium is not binary but ternary – that is to say, composed of a solvent, a solute and crystallization agents. During droplet contraction, both protein and crystallization agents concentrate and reach supersaturation. Then, for kinetic reasons,⁷⁶ salt crystallizes first and/or polymer induces an LLPS, often before protein nucleation. For these reasons, we use another experimental procedure to generate supersaturation for protein crystallization experiments, as described in the next section of the paper.

II.2. Confinement by fluxes. In this section, we describe how we use an external localized DC electric field to control the location of the nucleation event.

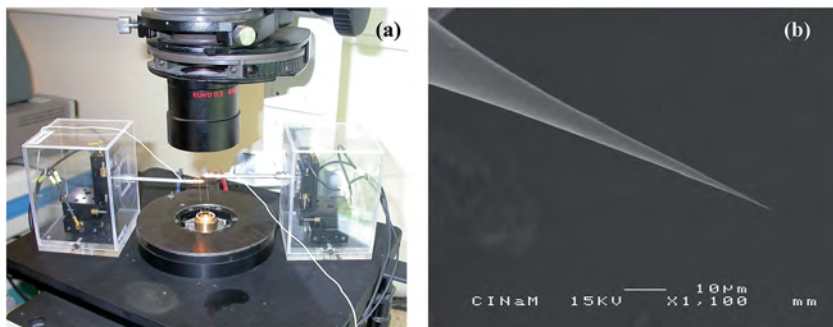


Fig. 7 (a) Temperature-controlled crystallization cell with the 2 micromanipulators and (b) SEM image of a W-tip.

Two electrodes were placed in a supersaturated metastable lysozyme solution (Fig. 7a), one of the electrodes being sharp (Fig. 7b). Because of the nanometer size of the tip, large electric fields⁷⁷ and large field gradients are encountered near the tip at low DC voltage. This geometry also induces a high current density inside the solution, close to the region of high curvature. Here, supersaturation was increased by a flux and an accumulation of molecules at a precise point in the vicinity of the tip apex.⁴¹ This accumulation created inside the crystallization cell a concentration gradient, that in solution is counteracted by convection. Therefore, the experiments were performed in gel in order to eliminate convection and keep the confinement in the vicinity of the electrode until the concentration reached the critical supersaturation.

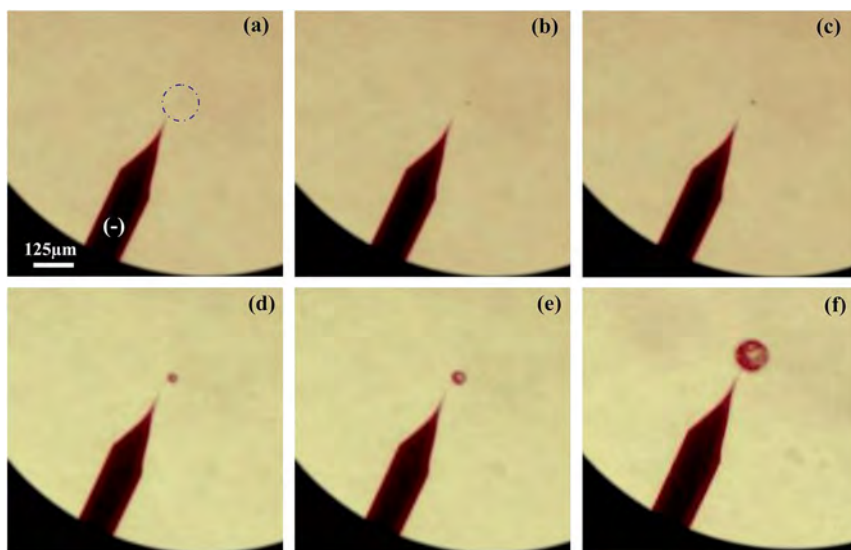


Fig. 8 Panels representing a time sequence showing nucleation and growth of lysozyme 20 mg mL^{-1} NaCl 0.7 M in agarose gel 1% (initial conditions: 0.5 V and $0.35 \mu\text{A}$) at (a) $t = 600 \text{ s}$, (b) $t = 1200 \text{ s}$, (c) $t = 1800 \text{ s}$, (d) $t = 7200 \text{ s}$, (e) $t = 10\,800 \text{ s}$ and (f) $t = 30\,000 \text{ s}$ (the (-) indicates the anode).

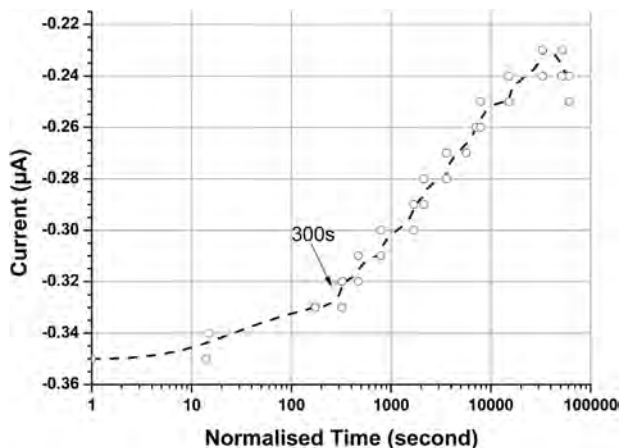


Fig. 9 Evolution of the current over time during the experiment, semi-log scale. Line is a guide for the eye.

The sequence presented in Fig. 8 shows that the use of gel as a crystallization medium clearly enables better control of the location of nucleation, and the nucleus appears in the vicinity of the cathode at the tip apex where the electric field is the strongest. As a result:

(1) The nucleation time in presence of the DC electric field is shorter than 600 s (instead of $t > 24$ h in the absence of an electric field); the nucleus is depicted by a circle in Fig. 8a.

(2) The particle is rough, due to high local supersaturation encountered during nucleation and growth.

(3) The average crystal growth rate (between 600 and 10 800 s) is $15 \mu\text{m h}^{-1}$, in agreement with the growth rate obtained by Durbin *et al.*⁷⁸ at high supersaturation for lysozyme.

(4) The current *vs.* time curve during the experiment clearly shows a modification in the slope at 300 s (Fig. 9), just before the nucleation becomes optically observable in Fig. 8a. Measuring current variation over time is thus a more sensitive way to detect nucleation than optical observation suggesting better control is expected. A theoretical study of the field nano-localization with alternating voltage is in progress in our group,⁷⁹ which should lead to a better understanding of the effect of the localized electric field on nucleation.

Conclusions

If all molecules follow the same rules⁸⁰ concerning crystallization, even though each material exhibits specific characteristics, the question is: do they have different nucleation mechanisms, as frequently proposed in the literature?

In this paper, we present different experimental approaches to study and control nucleation. The use of small volumes makes it possible to measure nucleation kinetics. We also show that coupling volume reduction with use of an external field makes it possible to obtain spatial and temporal control over nucleation for small molecules. Application to macromolecules raises some

difficulties; however, the use of an electric field to create localized field and fluxes shows promising results, leading to the spatial control of nucleation.

These experiments also shed light on some of the factors influencing the nucleation process.

Acknowledgements

We thank N. Ferte for protein characterization and fruitful discussions. We thank M. Sweetko for English revision.

References

- 1 D. Kashchiev, *Nucleation: basic theory with applications*, Butterworth-Heinemann, Oxford, 2000.
- 2 J. Gibbs, *The Collected Works, Vol. 1: Thermodynamics*, Yale University Press, 1948.
- 3 N. M. Dixit, A. M. Kulkarni and C. F. Zukoski, *Colloids Surf., A*, 2001, **190**, 47–60.
- 4 S. Selimovic, Y. Jia and S. Fraden, *Cryst. Growth Des.*, 2009, **9**, 1806–1810.
- 5 M. Ildefonso, N. Candoni and S. Veessler, *Cryst. Growth Des.*, 2013, **13**, 2107–2110.
- 6 O. Galkin and P. G. Vekilov, *J. Phys. Chem. B*, 1999, **103**, 10965–10971.
- 7 O. Galkin and P. G. Vekilov, *J. Am. Chem. Soc.*, 2000, **122**, 156–163.
- 8 T. Azuma, K. Tsukamoto and I. Sunagawa, *J. Cryst. Growth*, 1989, **98**, 371–376.
- 9 Y. Georgalis, A. Zouni and W. Saenger, *J. Cryst. Growth*, 1992, **118**, 360–364.
- 10 Y. Georgalis, A. Zouni, W. Eberstein and W. Saenger, *J. Cryst. Growth*, 1993, **126**, 245–260.
- 11 Y. Georgalis and W. Saenger, *Adv. Colloid Interface Sci.*, 1993, **46**, 165–183.
- 12 F. Boue, F. Lefaucheux, M. C. Robert and I. Rosenman, *J. Cryst. Growth*, 1993, **133**, 246–254.
- 13 A. J. Malkin and A. McPherson, *Acta Crystallogr., Sect. D: Biol. Crystallogr.*, 1994, **50**, 385–395.
- 14 N. Niimura, Y. Minezaki, M. Ataka and T. Katsura, *J. Cryst. Growth*, 1994, **137**, 671–675.
- 15 N. Niimura, Y. Minezaki, M. Ataka and T. Katsura, *J. Cryst. Growth*, 1995, **154**, 136–144.
- 16 N. Niimura, M. Ataka, Y. Minezaki and T. Katsura, *Phys. B*, 1995, **213 et 214**, 745–747.
- 17 Y. Minezaki, N. Niimura, M. Ataka and T. Katsura, *Biophys. Chem.*, 1996, **58**, 355–363.
- 18 N. Niimura, Y. Minezaki, I. Tanaka, S. Fujiwara and M. Ataka, *J. Cryst. Growth*, 1999, **200**, 265–270.
- 19 A. Stradner, H. Sedgwick, F. Cardinaux, W. C. K. Poon, S. U. Egelhaaf and P. Schurtenberger, *Nature*, 2004, **432**, 492–495.
- 20 J. B. Bishop, W. J. Fredericks, S. B. Howard and T. Sawada, *J. Cryst. Growth*, 1992, **122**, 41–49.
- 21 S. Veessler, S. Marcq, S. Lafont, J. P. Astier and R. Boistelle, *Acta Crystallogr., Sect. D: Biol. Crystallogr.*, 1994, **50**, 355.
- 22 M. Muschol and F. Rosenberger, *J. Cryst. Growth*, 1996, **167**, 738–747.

- 23 F. Rosenberger, P. G. Vekilov, M. Muschol and B. R. Thomas, *J. Cryst. Growth*, 1996, **168**, 1–27.
- 24 S. Finet, F. Bonnete, J. Frouin, K. Provost and A. Tardieu, *Eur. Biophys. J.*, 1998, **27**, 263–271.
- 25 M. Budayova-Spano, F. Bonnete, J. P. Astier and S. Veessler, *J. Cryst. Growth*, 2002, **235**, 547–554.
- 26 A. Shukla, E. Mylonas, E. Di Cola, S. Finet, P. Timmins, T. Narayanan and D. I. Svergun, *Proc. Natl. Acad. Sci. U. S. A.*, 2008, **105**, 5075–5080.
- 27 F. Bonneté, N. Ferte, J. P. Astier and S. Veessler, *J. Phys. IV*, 2004, **118**, 3–13.
- 28 H. N. W. Lekkerkerker, *Phys. A*, 1997, **244**, 227–237.
- 29 P. R. Ten Wolde and D. Frenkel, *Science*, 1997, **277**, 1975–1978.
- 30 V. J. Anderson and H. N. W. Lekkerkerker, *Nature*, 2002, **416**, 811–815.
- 31 D. Gebauer and H. Cölfen, *Nano Today*, 2011, **6**, 564–584.
- 32 P. G. Vekilov, *Cryst. Growth Des.*, 2004, **4**, 671–685.
- 33 D. Erdemir, A. Y. Lee and A. S. Myerson, *Acc. Chem. Res.*, 2009, **42**, 621–629.
- 34 D. Knezic, J. Zaccaro and A. S. Myerson, *J. Phys. Chem. B*, 2004, **108**, 10672–10677.
- 35 R. P. Sear, *CrystEngComm*, 2014, **16**, 6506–6522.
- 36 R. D. Dombrowski, J. D. Litster, N. J. Wagner and Y. He, *Chem. Eng. Sci.*, 2007, **62**, 4802–4810.
- 37 M. Ildefonso, N. Candoni and S. Veessler, *Org. Process Res. Dev.*, 2012, **16**, 556–560.
- 38 R. Grossier, Z. Hammadi, R. Morin, A. Magnaldo and S. Veessler, *Appl. Phys. Lett.*, 2011, **98**, 091916.
- 39 E. W. Muller and T. T. Tsong, *Field ion microscopy: principles and applications*, American Elsevier Publishing Company, New York, 1969.
- 40 Z. Hammadi, M. Gauch and R. Morin, *J. Vac. Sci. Technol., B: Microelectron. Nanometer Struct.–Process., Meas., Phenom.*, 1999, **17**, 1390–1394.
- 41 Z. Hammadi, J. P. Astier, R. Morin and S. Veessler, *Cryst. Growth Des.*, 2007, **7**, 1476–1482.
- 42 M. C. Robert and F. Lefaucheux, *J. Cryst. Growth*, 1988, **90**, 358–367.
- 43 S. Lee and J. Wiener, *J. Chem. Educ.*, 2010, **88**, 151–157.
- 44 M. Ildefonso, N. Candoni and S. Veessler, *Cryst. Growth Des.*, 2011, **11**, 1527–1530.
- 45 R. Grossier and S. Veessler, *Cryst. Growth Des.*, 2009, **9**, 1917–1922.
- 46 Z. Kozisek, K. Sato, S. Ueno and P. Demo, *J. Chem. Phys.*, 2011, **134**, 094508–094509.
- 47 D. Kashchiev, *J. Chem. Phys.*, 2011, **134**, 196102.
- 48 P. Laval, J.-B. Salmon and M. Joanicot, *J. Cryst. Growth*, 2007, **303**, 622–628.
- 49 L. Goh, K. Chen, V. Bhamidi, G. He, N. C. S. Kee, P. J. A. Kenis, C. F. Zukoski and R. D. Braatz, *Cryst. Growth Des.*, 2010, **10**, 2515–2521.
- 50 S. V. Akella, A. Mowitz, M. Heymann and S. Fraden, *Cryst. Growth Des.*, 2014, **14**, 4487–4509.
- 51 D. Tsekova, S. Dimitrova and C. N. Nanev, *J. Cryst. Growth*, 1999, **196**, 226–233.
- 52 E. Revalor, Z. Hammadi, J. P. Astier, R. Grossier, E. Garcia, C. Hoff, K. Furuta, T. Okutsu, R. Morin and S. Veessler, *J. Cryst. Growth*, 2010, **312**, 939–946.
- 53 P. B. Duncan and D. Needham, *Langmuir*, 2006, **22**, 4190–4197.
- 54 K. Allain, R. Bebawee and S. Lee, *Cryst. Growth Des.*, 2009, **9**, 3183–3190.
- 55 O. A. Bempah and O. E. Hileman Jr, *Can. J. Chem.*, 1973, **51**, 3435–3442.

- 56 J.-M. Ha, J. H. Wolf, M. A. Hillmyer and M. D. Ward, *J. Am. Chem. Soc.*, 2004, **126**, 3382–3383.
- 57 M. Beiner, G. T. Rengarajan, S. Pankaj, D. Enke and M. Steinhart, *Nano Lett.*, 2007, **7**, 1381–1385.
- 58 K. Kim, I. S. Lee, A. Centrone, T. A. Hatton and A. S. Myerson, *J. Am. Chem. Soc.*, 2009, **131**, 18212–18213.
- 59 C. J. Stephens, S. F. Ladden, F. C. Meldrum and H. K. Christenson, *Adv. Funct. Mater.*, 2010, **20**, 2108–2115.
- 60 R. Grossier, A. Magnaldo and S. Veessler, *J. Cryst. Growth*, 2010, **312**, 487–489.
- 61 I. Rodríguez-Ruiz, Z. Hammadi, R. Grossier, J. Gómez-Morales and S. Veessler, *Langmuir*, 2013, **29**, 12628–12632.
- 62 H. Langer and H. Offermann, *J. Cryst. Growth*, 1982, **60**, 389–392.
- 63 R. J. Davey, S. L. M. Schroeder and J. H. Ter Horst, *Angew. Chem. Int. Ed.*, 2013, **52**, 2166–2179.
- 64 Y. Kimura, H. Niinomi, K. Tsukamoto and J. M. García-Ruiz, *J. Am. Chem. Soc.*, 2014, **136**, 1762–1765.
- 65 E. M. Pouget, P. H. H. Bomans, J. A. C. M. Goos, P. M. Frederik, G. De With and N. A. J. M. Sommerdijk, *Science*, 2009, **323**, 1455–1458.
- 66 J. Baumgartner, A. Dey, P. H. H. Bomans, C. Le Coadou, P. Fratzl, N. A. J. M. Sommerdijk and D. Faivre, *Nat. Mater.*, 2013, **12**, 310–314.
- 67 B.-S. Lee, G. W. Burr, R. M. Shelby, S. Raoux, C. T. Rettner, S. N. Bogle, K. Darmawikarta, S. G. Bishop and J. R. Abelson, *Science*, 2009, **326**, 980–984.
- 68 S. T. Yau and P. G. Vekilov, *Nature*, 2000, **406**, 494–497.
- 69 U. Gasser, E. R. Weeks, A. Schofield, P. N. Pusey and D. A. Weitz, *Science*, 2001, **292**, 258–262.
- 70 M. Sleutel and A. E. S. Van Driessche, *Proc. Natl. Acad. Sci. U. S. A.*, 2014, **111**, E546–E553.
- 71 K.-Q. Zhang and X. Y. Liu, *Nature*, 2004, **429**, 739–743.
- 72 D. Voss, *Science*, 1996, **274**, 1325.
- 73 D. W. Oxtoby, *Nature*, 2002, **420**, 277–278.
- 74 D. Vivares, E. W. Kalera and A. M. Lenhoff, *Acta Crystallogr., Sect. D: Biol. Crystallogr.*, 2005, **61**, 819–825.
- 75 R. Grossier, Z. Hammadi, R. Morin and S. Veessler, *Phys. Rev. Lett.*, 2011, **107**, 025504.
- 76 A. A. Chernov, *Physics Reports I.M.Lifshitz and Condensed Matter Theory*, 1997, vol. 288, pp. 61–75.
- 77 R. Gomer, *Field emission and field ionization*, Harvard University press, Cambridge, 1961.
- 78 S. D. Durbin and G. Feher, *J. Cryst. Growth*, 1986, **76**, 583–592.
- 79 Z. Hammadi, R. Morin and J. Olives, *Appl. Phys. Lett.*, 2013, **103**, 223106.
- 80 A. A. Chernov, *J. Mater. Sci.: Mater. Electron.*, 2001, **12**, 437–449.